ATOMISTIC MODELING OF EXTENDED DEFECTS IN METALLIC ALLOYS - DISLOCATIONS AND GRAIN-BOUNDARIES IN L12 COMPOUNDS

ATOMISTIC MODELING OF EXTENDED DEFECTS IN METALIC ALLOYS: DISLOCATIONS AND GRAIN BOUNDARIES IN $L1_2$ COMPOUNDS

V. Vitek*, G. J. Ackland** and J. Cserti*
*Department of Materials Science and Engineering, University of Pennsylvania, Philadelphia, PA 19104, U.S.A.; ** Department of Physics, University of Edinburgh, Edinburgh, U.K.

ABSTRACT

Extended defects, such as dislocations and grain boundaries, control a wide variety of material properties and their atomic structure is often a governing factor. A necessary precursor for modeling of these structures is a suitable description of atomic interactions. We present here empirical many-body potentials for alloys which represent a very simple scheme for the evaluation of total energies and yet reflect correctly the basic physical features of the alloy systems modeled. As examples of atomistic studies we show results of calculations of the core structures of screw dislocations in $L1_2$ compounds. The same potentials have also been used to calculate structures of grain boundaries in these compounds. The deformation and fracture behavior of $L1_2$ alloys is then discussed in the light of grain boundary and dislocation core studies.

INTRODUCTION

Many physical properties of crystalline solids, in particular their mechanical behavior, are controlled by extended defects such as dislocations, grain boundaries and interfaces between different phases and materials. This is the reason why studies of the structure and behavior of such defects have been in the forefront of fundamental research in materials science for many years. While in some cases more macroscopic approaches, such as continuum mechanics analyses, suffice, in others it is the atomic structure and atomic level behavior of the defects which need to be understood. Examples of the former are the continuum theory of dislocations and fracture mechanics in the framework of which many important features of the mechanical behavior can be analyzed and understood. On the other hand, a wide variety of properties cannot be comprehended without studying the atomic structure of the defects concerned. The prime example are properties of interfaces which are controlled by the atomic structure in the very narrow region of their cores (see e.g. reviews [1,2] and proceedings of several recent symposia [3-5]). In the case of plastic deformation examples of phenomena which cannot be analyzed using the continuum theory of dislocations are the invalidity of the Schmid law observed in many materials other than f.c.c. metals, non-compact slip in h.c.p. materials, anomalous temperature dependences of the yield stress in intermetallic compounds etc. (see e.g. reviews [6-8]).

Most of the atomistic studies of extended defects have been made for pure metals, ionic crystals and semiconductors (see e.g. [9-14]) although understanding of the atomic structure of crystal defects in alloys is even more important. Two examples of atomic level phenomena crucial for microscopic understanding of the mechanical properties of materials are segregation to grain boundaries and interfaces in disordered alloys, and dislocation core behavior and intrinsic grain boundary brittleness in intermetallic compounds. The main reason why studies of

extended defects in alloys are still relatively rare is the lack of reliable descriptions of atomic interactions in alloys.

For pure metals the description of interatomic forces used in defect studies ranges from empirical and pseudopotential theory based pair-potentials (for reviews see [15-17]), through N-body potentials and the embedded atom method (EAM) [18-21] to tight-binding methods (see e.g. papers by Andersen, Pettifor, Paxton, Legrand, Finnis and Haydock in Ref. [14]) and ab-initio non-central potentials [22,23]. For alloys ab-initio pair-potentials have been derived for some binary systems with weak electron-ion pseudopotentials [17] and several attempts have been made to describe interatomic forces in terms of empirical pair-potentials (see e.g. [24-26]). In the framework of pair-potentials usually used in studies of defects the energy of an assembly of N atoms is given as

$$E = \frac{1}{2} \sum_{i \neq j=1}^{N} V_{ij}(R_{ij}) + U(\rho) \qquad (1)$$

where V_{ij} is the pair potential describing the interaction between the atoms of the type i and j, respectively, separated by the the distance R_{ij}, and $U(\rho)$ is the density dependent part of the energy; ρ is the average density of the alloy. Such pair potentials belong to the class of *constant volume* potentials [22] and may reasonably describe the energy changes associated with the variation of atomic configurations at constant volume. For this reason most of the calculations using such potentials have been made at constant volume. However, in alloys the difference between the atomic sizes of constituent species is an important parameter and local density variations need to be taken into account. In principle this can be done by regarding ρ as the local density, but owing to the uncertainties of evaluation of this quantity as well as applicability of the density dependent term on the local level, this extension of the use of pair-potentials is rather cumbersome (see e.g. [25]). However, this problem has been overcome in the recent developments of the EAM and N-body potentials. In the framework of these schemes the energy of the system of N atoms is

$$E = \frac{1}{2} \sum_{i \neq j=1}^{N} V_{ij}(R_{ij}) - \sum_{i=1}^{N} F_i(\rho_i) \qquad (2)$$

where F_i is the many body and/or embedding part of the energy which replaces $U(\rho)$ and its form is chosen on the basis of more fundamental physical considerations [18,19]. ρ_i, which can be identified with the electron density in the Wigner-Seitz cell associated with the atom i, is written as $\rho_i = \sum_j \Phi_j(R_{ij})$. Both V_{ij} and Φ_j are pair-potentials.

In this paper we first summarize a recently developed procedure for construction of N-body potentials for binary alloys [27] which employs the Finnis-Sinclair type many-body potentials [19]; the energy of the system is given by equation (2) with the function F_i taken as a square root. A justification for this form of the many-body function is provided in the framework of a second moment approximation of the density of states to the tight-binding theory incorporating local

large conservation [28]. Since the constructed potentials are to be used for studies of extended defects in given crystal structures these potentials have to satisfy certain stability conditions and the requirements imposed on the potentials representing specific alloys, as well as on the potentials representing model materials, are discussed here. Potentials for Cu-Au and Ni-Al alloys are then presented and applied in calculating the dislocation core structure in $L1_2$ compounds Ni_3Al and Cu_3Au. In our previous studies these potentials have also been used to model grain boundaries in these alloys [29, 30]. Dislocation core structures calculated using a model potential exhibiting an $L1_2$ compound with a very high antiphase boundary (APB) energy and unstable complex stacking faults (CSF) on (111) planes, are also shown. The deformation and fracture behavior of $L1_2$ compounds is discussed in the light of the results of these atomistic studies.

REQUIREMENTS FOR DESCRIPTIONS OF INTERATOMIC FORCES

Conditions which have to be satisfied by potentials used in atomistic studies of extended lattice defects follow to a great extent from the goal of these calculations. The principal purpose of such investigations is to elucidate the atomic structure and atomic level properties of lattice defects in alloys with given:

(i) *Crystal structures.*
(ii) *Alloying properties, characterized, for example, by alloying and ordering energies.*
(iii) *Elastic properties and, possibly, phonon spectra.*
(iv) *Values of certain material parameters such as stacking fault and anti-phase boundary energies, vacancy formation energies, energies of anti-site defects .*

Hence, when constructing such potentials the aim is not to predict the above material properties but to reproduce them. This is in contrast with theoretical studies of alloy formation the objective of which is to determine these properties from first principles.

When reproducing the above properties equilibrium data are used but the potentials are then employed in calculations of structures in which large distortions of the local environment away from equilibrium are present. This raises an important question of the transferability of the potentials which is not necessarily guaranteed by reproduction of equilibrium properties. While the extent of transferability of empirically constructed potentials cannot be deduced from any general arguments, it is likely to be wide enough if the potentials constructed for a given alloy system ensure:

(i) *The stability of the appropriate crystal structure relative to alternate structures with different symmetry or chemical order.*
(ii) *The mechanical stability of this structure relative to both small and large homogeneous deformations.*
(iii) *Reproducibility of the basic features of the phase diagram.*

The reason is that unphysical structural or ordering instabilities are then much less likely to occur in the cores of extended defects. Nevertheless, the validity of the structural features of lattice defects found in calculations using such potentials is best guaranteed if they can be related to fitted material properties and do not arise from those characteristics of the potentials which are not well justified within the scheme employed.

However, in many atomistic studies the purpose of the research is not to investigate a specific alloy but rather to examine the effect of certain physical parameters upon crystal defects in specific structures. Potentials constructed for this purpose do not represent then any particular material but mechanically and chemically stable structures of the same type with varying values of a chosen parameter. As an example we present below a N-body potential leading to a stable $L1_2$ structure in which the CSF on {111} planes is unstable and demonstrate the consequence of this instability for the core structure of screw dislocations.

N-BODY POTENTIALS FOR BINARY ALLOYS

The N-body potentials have been constructed within the Finnis-Sinclair [19] scheme where the energy associated with an atom **i** in a system of N atoms is

$$E_i = \sum_{j=1}^{N} V_{ij}(R_{ij}) - \sqrt{\sum_{j=1}^{N} \Phi_{ij}(R_{ij})} \tag{3}$$

where the suffices ij of the pair-potentials V and Φ refer to the species of the atoms involved. For the binary systems these potentials are denoted V_{AA}, V_{AB}, V_{BB}, Φ_{AA}, Φ_{AB}, and Φ_{BB}. Functions V_{AA}, V_{BB}, Φ_{AA}, and Φ_{BB} were identified with those for pure metals. The function Φ_{AB} was chosen as a geometrical mean of Φ_{AA} and Φ_{BB}. This is consistent with its interpretation in terms of hopping integrals, and minimizes the empirical fitting. Hence, only the pair potential V_{AB} needs to be fitted to alloy properties.

For consistency with the functional forms used for the pure materials [20], we employed cubic splines for V_{AB}. so that the functions which make up the present model are:

$$\begin{aligned}
V_{AA}(R_{ij}) &= \sum_{k=1}^{6} a_k^{AA} H(r_k^{AA} - R_{ij})(r_k^{AA} - R_{ij})^3 \\
\Phi_{AA}(R_{ij}) &= \sum_{k=1}^{6} A_k^{AA} H(R_k^{AA} - R_{ij})(R_k^{AA} - R_{ij})^3 \\
V_{AB}(R_{ij}) &= \sum_{k=1}^{4} a_k^{AB} H(r_k^{AB} - R_{ij})(r_k^{AB} - R_{ij})^3 \\
\Phi_{AB}(R_{ij}) &= \sqrt{\Phi_{AA}(R_{ij})\Phi_{BB}(R_{ij})}
\end{aligned} \tag{3}$$

where $H(x)$ is the Heavyside step function. The parameters a_k^{AA}, A_k^{AA}, r_k^{AA} and R_k^{AA} are summarized in Table 1 for Cu, Au, Ni and Al. Parameters a_k^{AB} and r_k^{AB} for the three alloy systems discussed here, are summarized in Table 2. For pure metals these coefficients are given in a normalized form, but for alloys there is no unique lattice parameter for all concentrations with respect to which one can define the

coefficients, so in Table 2 we use absolute units of Å and eV/Å3 for r_k^{AB} and a_k^{AB}, respectively.

	Copper	Gold	Nickel	Aluminum
a_1	61.73525861	29.059066	32.9100	32.2588
a_2	-108.18467800	-153.14779	-51.3477	-74.5610
a_3	57.00053948	148.17881	39.2079	140.0125
a_4	-12.88796578	-22.20508	-88.2142	-107.5789
a_5	39.16381901	72.71465	131.1403	29.4447
a_6	0.0000000	199.26269	0.0000	0.0000
A_1	10.03718305	21.930125	28.7717	19.2224
A_2	17.06363299	284.99631	-94.0309	4.9595
r_1	1.225	1.2247449	1.225	1.225
r_2	1.202	1.1547054	1.202	1.180
r_3	1.154	1.1180065	1.100	1.090
r_4	1.050	1.0000000	0.900	1.050
r_5	0.866	0.8660254	0.820	0.900
r_6	0.707	0.7071068	0.707	0.707
R_1	1.225	1.1180065	1.225	1.200
R_2	0.990	0.8660254	0.930	0.930
a(Å)	3.615	4.078	3.524	4.050

Table 1. Parameters of many-body potentials for copper, gold, nickel and aluminum

	Copper - Gold	Nickel - Aluminum	$L1_2$ with unstable CSF
r_1	4.309816	4.35174	4.35174
r_2	4.047479	4.24473	4.24473
r_3	3.297946	3.88803	3.88803
r_4	0.000000	2.96061	2.96061
a_1	-0.0855455166	-0.6469208776	2.4706946660
a_2	0.192835880	1.1392692848	-3.5210921605
a_3	0.75932286	-0.6655106072	1.1973534670
a_4	0.0000000	1.4680219296	0.9745088396

Table 2. Parameters for potentials V_{AB}

In the case of the Cu-Au system the potential for Au is the same as in [20] but the potential for Cu has been re-derived to eliminate the 'bump' in the pair-potential

between second and third neighbors [27]. The potential V_{AB} was fitted to reproduce the alloying energies in disordered alloys for given concentrations c_{Cu} and c_{Au} as

$$E^{alloy} = E^{rand} - c_{Cu}E^{Cu} - c_{Au}E^{Au} \quad (4)$$

where E^{Cu} and E^{Au} are energies per atom in pure Cu and Au, respectively, and E^{rand} is the energy per atom in the random alloy. The available experimental data on alloying energies correspond to high temperatures while no temperature effects are taken into account in fitting procedures. Hence, we assume that the alloying energy is independent of temperature below the melting point. In previous works (e.g. [25,31]) the energy of a single substitutional atom has been used for empirical fitting of alloying energies. However, experimental data for single substitutional atoms does not exist as such but it is usually extrapolated from a region of about 10% concentration. At this concentration 72% of impurity atoms have at least one impurity as a nearest neighbor (based on a random distribution of species in an f.c.c. lattice). Furthermore, the relaxation of the lattice around the substitutional atom can be significant and the nature of this relaxation will depend on the concentration. Therefore, V_{AB} has been fitted to observed random alloy formation energies at finite concentrations, tabulated in [32], taking the atomic relaxation into account. Furthermore, the lattice parameter for the $L1_2$ ordered Cu_3Au alloy was fitted since the potentials are intended for studies of lattice defects in this alloy. The details of the corresponding fitting procedures are described in [27].

The results of the fitting for Cu-Au alloys are seen in Fig. 1 which shows the experimental and calculated alloying energies for various alloy concentrations. The calculations were carried out using a molecular statics relaxation method and a large variety of possible configurations for each concentration (for details see [27]). The experimental values are reproduced very well for copper concentrations larger than 50% but for gold rich alloys the calculated values are lower than the experimental ones. This means that in the latter case the calculated local relaxations are more extensive than in the real alloy. However, a short range order is likely to exist in reality even at high temperatures which suppresses the relaxation, while the fitting was carried out assuming an ideally disordered alloy.

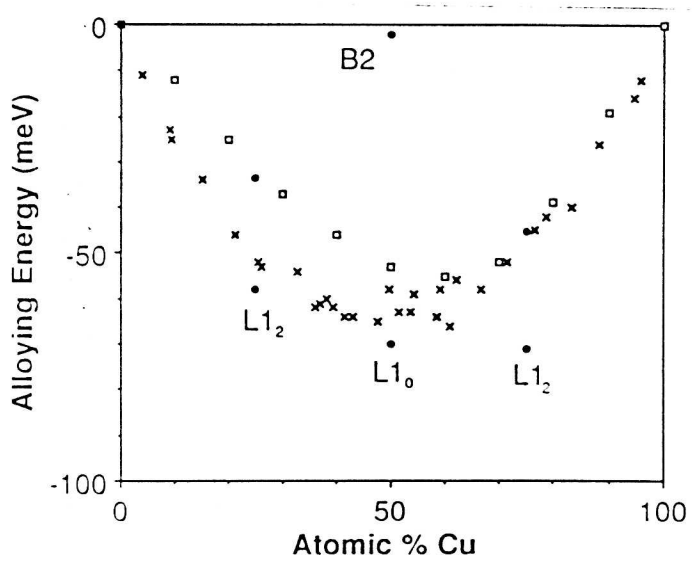

Fig. 1. Concentration dependence of the alloying energy in copper-gold. Open circles: experiment; crosses: molecular statics calculations; filled circles: ordered alloys.

The alloying energies of $L1_2$ Cu_3Au and Au_3Cu alloys, as well as of the $L1_0$ and B2 CuAu alloys are also shown in Fig. 1. The energies of $L1_2$ and $L1_0$ are lower than those of the corresponding disordered alloys and, therefore, these ordered structures are favoured at low temperatures over the disordered phase and in the case of CuAu over the B2 structure. Hence, the potentials reproduce, without any further adjustment, the basic features of the phase diagram of this alloy system [32]. We have not calculated the order-disorder transition temperatures since this depends very sensitively on both the ordering energies and the treatment of the entropy which should incorporate possible short range order in the disordered state. However, we have evaluated the energy of the 1/2<110> APB on {111} planes in Cu_3Au, which is a more global quantity principally controlled by the ordering energy. Its value, given in Table 3 together with the energies of other planar faults in this alloy, compares well with the experimental estimates of 40-60 mJm^{-2} [33, 34].

In the case of Ni-Al system the potentials for Ni and Al were constructed using the same method as in the case of Cu and Au, which was described in detail in Ref. [20]. The physical quantities fitted are the cohesive energy, the equilibrium lattice parameter for the f.c.c. structure, the elastic constants and the vacancy formation energy. It should be noted that the potential for Ni used here differs somewhat from that given in [20] and does not reproduce the stacking fault energy. The potential for Al constructed here is of the same type as those for the noble metals and Ni and thus the corresponding effective pair-potential [19, 20] has such a form that the first nearest neighbors are on its repulsive side and the second nearest neighbors on its attractive side. This is in contrast with the ab-initio pair potential for Al for which both the first and second nearest neighbors are on the repulsive side; this feature of the potential arises due to the very high density of electrons in Al [35]. Thus the constructed N-body potential for Al may be appropriate in alloys containing Al since the electron density in these alloys is much lower than in the pure Al but should be used with caution for pure Al.

The potential V_{AB} was fitted in the case of Ni-Al such as to reproduce for $L1_2$ (Ni_3Al) and B2 (NiAl) structures the alloying energies (4.57eV and 4.39eV, respectively) and lattice parameters (3.567Å and 2.88Å, respectively) as well as, approximately, the elastic constants for the $L1_2$ structure (c_{11} = 2.4x10^{11}Pa, c_{12} = 1.5x10^{11}Pa, c_{44} = 1.26x10^{11}Pa). Furthermore, the energy of the 1/2<110> APB on {111} planes was fitted so that it is close to the value estimated experimentally [36]. Its value, together with energies of other planar faults, are given in Table 3. Finally, the stability of $L1_2$ and/or B2 structures relative to other possible structures (DO_{19}, DO_{22}, A15, $L1_0$) was tested.

	Cu_3Au	Ni_3Al	$L1_2$ with unstable CSF
APB on {111}	54	226	770
APB on {001}	52	53	338
CSF	40	189	Unstable
SISF	15.6	11.4	13.3

Table 3. Energies (in mJm^{-2}) of the APBs on {111} and {001} planes and the complex (CSF) and superlattice intrinsic (SISF) stacking faults on {111} planes.

When constructing the N-body potentials which lead to an unstable complex stacking fault (CSF) in the $L1_2$ structure, the V_{AA} and V_{BB} potentials are those for Ni and Al. Similarly, the potential V_{AB} was fitted to the same quantities as when constructing the potentials for Ni-Al system but the value of the APB energy on {111} planes was adjusted to be very high (see Table 3). This is equivalent to choosing a very high ordering energy and, as shown in our earlier studies [37-39], this may lead to the instability of both the APB and CSF. In the present case only the CSF is not stable.

DISLOCATION CORES IN $L1_2$ ORDERED ALLOYS

Ni_3Al and Cu_3Au

Nickel based $L1_2$ compounds, such as Ni_3Al, show a number of unusual features when deformed at temperatures between 300° and 1000° K. The most remarkable are the increase of the flow stress with increasing temperature and strong dependences of the yield stress on the orientation of the tensile axis, accompanied by tension-compression asymmetries (see e.g. [40, 41]). It is now generally accepted that this behavior results from special features of the cores of <110> screw dislocations [6-8, 41, 42]. At the same time alloys like Cu_3Au do not exhibit any orientation dependences of the yield stress while in platinum based alloys, such as Pt_3Al, the yield stress increases rapidly with decreasing temperature but there are no anomalous temperature dependences at high temperatures [43-45]. In the latter case the deformation behavior can again be explained by dislocation core properties [6, 46]. Atomistic studies of the core structure of <110> screw dislocations have been carried out in the past using pair-potentials [6, 37, 39]. Present calculations fully confirm these results but also demonstrate the existence of an important core configuration which was previously assumed [42] but not revealed by direct atomistic simulations.

Calculations employing the N-body potentials for Ni_3Al and Cu_3Au were carried out for superdislocations dissociated either on the (111) or on the (001) plane according to the reaction $[1\bar{1}0] = 1/2[1\bar{1}0] + 1/2[1\bar{1}0]$ with the corresponding APB in between the superpartials. They were performed using a gradient relaxation technique utilizing periodic boundary conditions in the direction of the dislocation line ($[1\bar{1}0]$). The dimensions of the relaxed block in the two directions perpendicular to the dislocation line ($[11\bar{2}]$ and [111]) were $50a$, where a is the lattice parameter, so that the block contained 14210 atoms. The atoms in the outer region, the size of which is determined by the cut-off of the interatomic forces, were held at fixed positions evaluated in accordance with the anisotropic elastic displacement field of the dislocation studied. In the following the calculated core structures are interpreted using the method of differential displacements commonly utilized in dislocation core studies (see e.g. [8, 47]). The atomic arrangement is shown in the projection onto the $(1\bar{1}0)$ plane. Small circles represent the A atoms, and large circles the B atoms of the A_3B alloy. Two consecutive $(2\bar{2}0)$ planes are always shown and distinguished by darkly and lightly shaded circles. The $[1\bar{1}0]$ (screw) component of the relative displacement of the neighboring atoms produced by the

dislocation is depicted as an arrow between them. The length of the arrows is proportional to the magnitude of the displacement and it is normalized modulo $|1/2[1\bar{1}0]|$. The direction of the arrow represents the sign of the displacement. In this scheme rows of arrows of constant length mark planar faults such as APBs.

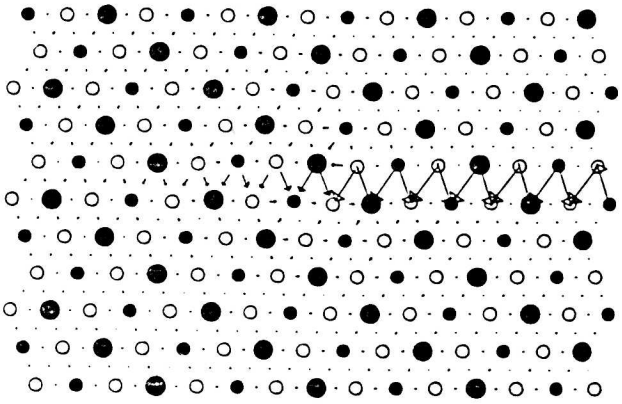

Fig. 2.

$1/2[1\bar{1}0]$ superpartial in Ni_3Al bounding the APB on the (111) plane: Glissile configuration.

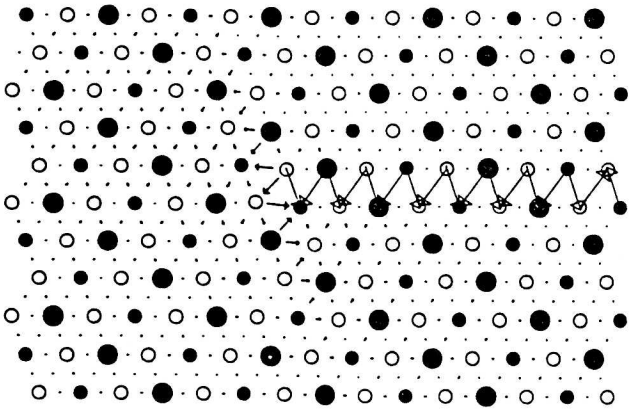

Fig. 3.

$1/2[1\bar{1}0]$ superpartial in Ni_3Al bounding the APB on the (111) plane: High energy sessile configuration.

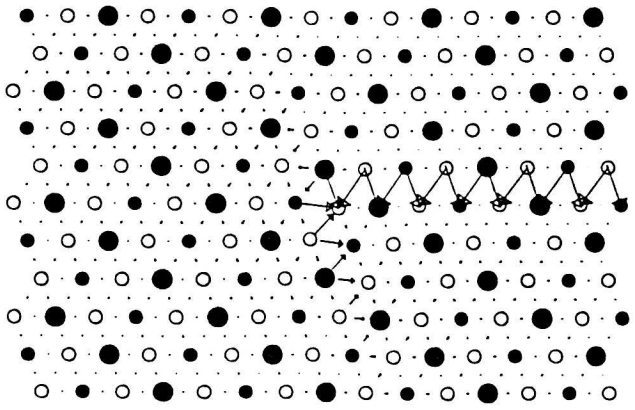

Fig. 4.

$1/2[1\bar{1}0]$ superpartial in Ni_3Al bounding the APB on the (111) plane: Low energy sessile configuration.

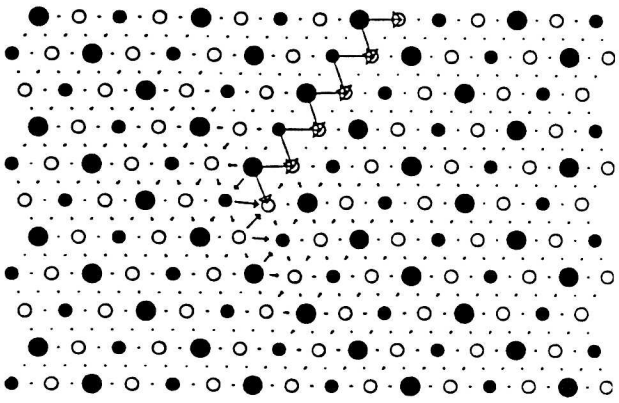

Fig. 5.

$1/2[1\bar{1}0]$ superpartial in Ni_3Al bounding the APB on the (001) plane.

In the case of Ni_3Al three different core configurations of the $1/2[1\bar{1}0]$ superpartial, shown in Figs. 2 - 4, were found when the APB is on the (111) plane. Two symmetry related configurations, one of which is shown in Fig. 5, were found when the APB is on the (001) plane. In Fig. 2 the core is spread in the plane of the APB and, therefore, this configuration is glissile. On the other hand, in Figs. 3 - 5 the cores are extended into the $(1\bar{1}1)$ plane while the APBs are either on the (111) or

the (001) plane. Hence, these configurations are sessile. A common feature of all the four configurations is spreading of the dislocation core into one of the {111} planes which. This core spreading, although very narrow, can be described to a good approximation as dissociation into 1/6<112> type Shockley partials.

Structures shown in Figs. 2, 3 and 5 were found in the former pair-potential calculations [37] as well as in the recent calculations employing the EAM [48, 49]. However, the core structure shown in Fig. 4 has not been found in previous atomistic studies. When this structure is compared with that shown in Fig. 5, a close resemblance of the core displacements is obvious. Hence, it can be interpreted as consisting of a narrow strip of the (001) APB, approximately | 1/4[110] | wide, connecting the APB on the (111) plane with the dislocation spread into the $(1\bar{1}1)$ plane. The assumption that such a sessile core configuration exists is an essential ingredient in the theoretical analysis of the origin of the yield stress anomaly and its orientation dependences in $L1_2$ compounds [42]. In this model cores of glissile screw dislocations transform into the above configuration by a cross-slip type mechanism and create thus intrinsic obstacles for the subsequent motion of these dislocations. The main driving force for this process is the lower energy of the sessile configuration related to the lower energy of the APB on {001} planes.

The division of the dislocation energy into the core and elastic parts is not unique and in a large block the elastic energy dominates. To make an assessment of the energy differences between different core configurations we evaluated for each case the energy of a small block of atoms (240) centered on the corresponding core; in each case the ratio of Ni and Al atoms in this block is 3:1. The ratio of the energies for the three cases shown in Figs. 2, 3 and 4 are 1 : 1.03 : 0.95. Clearly, the sessile configuration of Fig. 4 is energetically the most favorable as assumed in [42]. The other sessile core is a higher energy configuration.

Calculations using the potentials for Cu_3Au revealed configurations analogous to those shown in Figs. 2, 3 and 5 with clearly defined dissociation into the Shockley partials. However, the structure analogous to that of Fig. 4 has not been found. This is consistent with the above interpretation of this core structure. In the case of the potentials for Ni_3Al the APB energy on {001} planes is much lower than on {111} planes but these energies are very similar in the case of the potentials for Cu_3Au. Hence, in the latter case formation of an atomic size ribbon of the (001) APB does not necessarily lower the energy of the core.

Model material with unstable CSF

Similarly as in the previous cases, the dissociation of the <110> superdislocations into two 1/2<110> superpartials may occur on {001} planes but owing to the very high APB energy on {111} planes, it cannot take place on these planes [37]. Instead, the superdislocation may dissociated on the (111) plane according to the reaction $[1\bar{1}0] = 1/3[1\bar{2}1] + 1/3[2\bar{1}\bar{1}]$ with the SISF in between the superpartials. Both the core structure of the $1/2[1\bar{1}0]$ superpartial bounding the APB on the (001) plane and of the $1/3[1\bar{2}1]$ superpartial bounding the SISF on the (111) plane were studied. The calculations were carried out in the same way as described above and the results are shown in Figs. 6 and 7, respectively.

It is seen from Fig. 6 that the core of the $1/2[1\bar{1}0]$ superpartial is not confined to the (001) plane but spreads *simultaneously* into both the (111) and $(1\bar{1}1)$ planes. Thus

the core is again sessile. However, it cannot be interpreted as splitting into two Shockley partials since the CSF is not stable. This is, of course, the reason why the core now spreads symmetrically into two different {111} planes. Since the $1/3[1\bar{2}1]$ superpartial possesses an edge component, significant displacements perpendicular to the $[1\bar{1}0]$ direction exist in its core but only the screw component of the displacements is shown in Fig. 7. These displacements are again spread simultaneously into the (111) plane, one layer above the plane of the SISF, and to the $(1\bar{1}1)$ plane. The edge component of the displacements remains in the plane of the SISF. Thus the core of this superpartial is again sessile and its screw component has the same form as the core of the $1/2[1\bar{1}0]$ superpartial shown in Fig. 6. These results are practically the same as those obtained earlier using model pair-potentials [37, 39].

As explained earlier, the model N-body potential was not constructed to describe any specific alloy but rather a class of materials in which the APB energy on {111} planes is so high that the usual dissociation into $1/2[1\bar{1}0]$ superpartials cannot take place on these planes and, furthermore, the CSF is not stable. The results of the dislocation core calculations show that if such $L1_2$ compounds exist, their plastic behavior will be very different from that of compounds like Ni_3Al or Cu_3Au. The main reason is that there is now no glissile configuration of the screw dislocation core and thus movement of these dislocations will always be impeded, similarly as, for example, in b.c.c. metals [6, 8, 47]. Since the motion of sessile dislocations can be aided by thermal activations the yield stress will be decreasing with the increasing temperature but no intrinsic reason for high temperature anomalies exist. Furthermore, since the sessile part of the core structure is practically the same whether the superdislocation is on {111} or {001} planes, the slip may occur on either of these planes, principally in dependence on the corresponding Schmid factor. Such a model was found to explain very closely the plastic properties of Pt_3Al [45, 46].

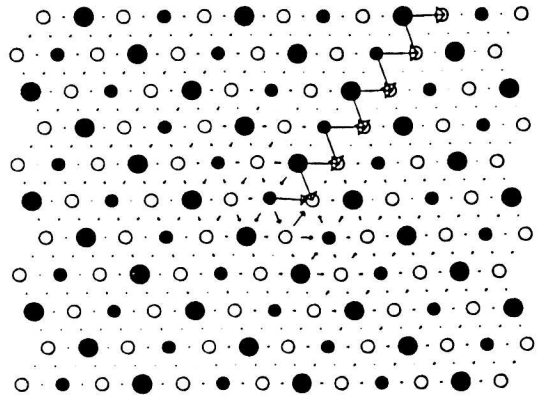

Fig. 6.

$1/2[1\bar{1}0]$ superpartial in the model material bounding the APB on the (001) plane.

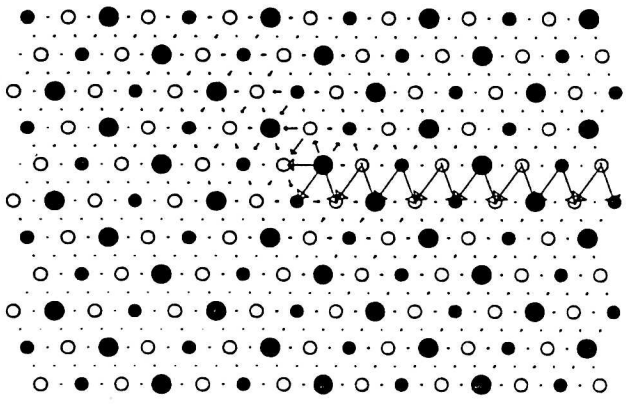

Fig. 7.

$1/3[1\bar{2}1]$ superpartial in the model material bounding the SISF on the (111) plane.

GRAIN BOUNDARY STRUCTURE IN NI_3AL AND CU_3AU

A remarkable feature of grain boundaries in some $L1_2$ intermetallic compounds, for example Ni_3Al, is their intrinsic brittleness [50-52]. In contrast, grain boundaries in disordered alloys are not generally susceptible to brittle cracking and when intergranular fracture occurs it is usually associated with segregation of embrittling impurities to grain boundaries (see e.g. [53, 54]). Similarly, Cu_3Au which also possesses the $L1_2$ structure, is always ductile. In order to elucidate the fracture properties of grain boundaries in $L1_2$ alloys atomic structures of several grain boundaries have been modelled using the N-body potentials for Ni_3Al and Cu_3Au and more details can be found in Refs. [29, 30].

The principal distinction between Ni_3Al and Cu_3Au which is reflected in the potentials, is a large difference in the ordering energies. Cu_3Au is a weakly ordered alloy with an order-disorder transformation well before melting while Ni_3Al is a strongly ordered compound which stays ordered up to melting. The ordering propensities are reflected in the energies of APBs (see Table 2). The results of the atomistic calculations of grain boundaries show that in Ni_3Al all the atoms in the boundary region can be regarded as uniquely attached to either the upper or the lower grain so that the ideal $L1_2$ structure is almost undisturbed on either side of the boundary up to the boundary plane. Hence only very small local relaxation of atoms in the boundary region takes place. The same structural features were found when using pair potentials [55] and can be seen in the results of all the EAM calculations [56, 57]. On the other hand, in Cu_3Au, and also in pure f.c.c. metals, the relaxation in the boundary is considerable and in a narrow region of the boundary the atoms cannot be clearly assigned to either the upper or the lower grain.

The reason for these structural differences are very different ordering energies in the two alloys. In the case of Ni_3Al the chemical order is the principal factor controlling the energy of the system. Its preservation dominates the grain boundary structure and results in lack of the local atomic relaxation in the boundary region which then leads to the presence of columnar cavities in grain boundaries in Ni_3Al. On the other hand, in the case of Cu_3Au more relaxed grain boundary structures, similar to those in pure f.c.c. metals, are energetically favored over those in which the order is preserved at the expense of a significant inhomogeneity in the boundary region.

The cavities in grain boundaries in Ni_3Al may serve as nucleation sites for microcracks. Furthermore, the plastic relaxation in the boundary region may be more difficult in strongly ordered alloys. The reason is that if the ideally ordered $L1_2$ structure extends up to the boundary a high energy APB is formed during plastic shearing in this region. On the other hand, in weakly ordered alloys the region of the boundary may be structurally, and also chemically, disordered so that no APB is formed during the localized shearing and even if the order is preserved, the energy of the corresponding APB is much lower. Similarly, the transmission of the dislocations through the boundary is likely to be easier in the disordered case as suggested in [58, 59]. The calculated atomic structures of grain boundaries thus suggest that nucleation and subsequent propagation of intergranular cracks in strongly ordered $L1_2$ alloys is much easier than either in pure f.c.c. metals or in weakly ordered alloys.

DISCUSION

Descriptions of interatomic forces required for atomistic studies of extended defects need to be sufficiently simple so that relaxation calculations involving hundreds or thousands of atoms may be carried out. At the same time they have to be adequately justified physically and fulfill conditions for the mechanical and structural stability of the crystal structure in which the defects are investigated. However, they do not have to predict the structural and energetic characteristics of the defect free state, such as phase stabilities, lattice parameter, elastic properties. Rather, these properties are used as fitting parameters in the construction of the corresponding potentials. For this purpose both the N-body potentials of the Finnis-Sinclair type and the EAM method are very suitable schemes which represent an important improvement upon the empirical pair-potentials in that the density dependent part of the energy is an explicit function of the atom positions.

In general two different routes can be followed when constructing such potentials. First are the potentials representing specific materials and ensuing atomistic studies then relate the defect properties and behavior to certain basic characteristics of the given material. Second are the potentials which do not represent any particular material but model materials with varying values of chosen parameters and the purpose of the atomistic studies is then to investigate the influence of these parameter on the defect properties for a chosen class of materials. An example of the former are the N-body potentials for Cu-Au and Ni-Al systems and of the latter the model N-body potentials for $L1_2$ structures with very high APB energy and unstable CSF on {111} planes. In this paper we have employed both types of potentials in atomistic calculations of the core structure of <110> screw superdislocations in $L1_2$ alloys.

Calculations employing potentials for Ni-Al and Cu-Au systems have revealed glissile and sessile forms of the core of 1/2<110> screw superpartials for both Ni_3Al and Cu_3Au. The low energy sessile core structure (Fig. 4) in Ni_3Al can be identified with the configuration assumed in the theoretical analysis of the anomalous behavior of the yield stress at high temperatures [42]. The same core structure has not been found in Cu_3Au. This is consistent with the fact that the dislocation core controlled anomalous increase of the yield stress with temperature, characterized by strong orientation dependences, is observed in Ni_3Al but not in Cu_3Au.

When using the same potentials in studies of grain boundaries, important structural differences between Ni_3Al and Cu_3Au were found. These are directly related to the strength of ordering and may explain the intrinsic grain boundary brittleness of strongly ordered compounds such as Ni_3Al.

The model calculations have shown that if the APB energy on {111} planes in a $L1_2$ compound is so high that the splitting into 1/2<110> superpartials cannot take place on these planes, the <110> superdislocations are always sessile whether dissociated on a {001} plane with the APB or on a {111} plane with the SISF. The yielding behavior of such a material is then entirely different than that of either Ni_3Al or Cu_3Au and, as already shown in our earlier studies, this model situation explains the temperature and orientation dependences of the yield stress in Pt_3Al. Thus it is proposed that in this compound the APB energy on {111} planes is unusually high, and this determines its very different yielding behavior when compared with many other $L1_2$ alloys. However, this suggestion can only be proved by more fundamental quantum mechanical calculations.

ACKOWLEDGEMENTS

This research was supported by the NSF Grant No. DMR88-22858 and the NSF MRL Program DMR88-19885 (GJA).

REFERENCES

1. A. P. Sutton, Int. Metals Reviews **29**, 136 (1984).
2. V. Vitek, in Dislocations 1984, edited by P. Veyssiere, L. Kubin and J. Castaign (CNRS Press, Paris, 1984), p.435.
3. Grain Boundary Structure and Related Phenomena, Trans. Japan Inst. Metals **27** (1986)
4. Interfacial Structure, Properties and Design, edited by M. H. Yoo, W. A. T. Clark and C. L. Briant (Mater. Res. Soc. Proc., Vol. **122**, Pittsburgh, PA, 1988).
5. Interface Science and Engineering, edited by R. Raj and S. L. Sass, J. Phys. Paris **49** (1988).
6. V. Vitek, in Dislocations and Properties of Real Materials, edited by M. H. Loretto (The Institute of Metals, London, 1985), p. 30.
7. P. Veyssiere, Rev. Phys. Appl. Paris **23**, 673 (1988).
8. M. S. Duesbery, in Dislocations in Solids, edited by F. R. N. Nabarro (Elsevier Science Publ., Amsterdam, 1989), p. 67.
9. Interatomic Potentials and Lattice Defects, edited by J. K. Lee (The Metallurgical Society of AIME, Warrendale , PA, 1981).
10. Computer Simulation of Condensed Matter, edited by C. R. A. Catlow and W. C. Mackrodt, Physica B+C **131**, Nos. 1-3 (1985).
11. Computer-Based Microscopic Description of the Structure and Properties of Materials, edited by J. Broughton, W. Krakow and S. T. Pantelides (Mater. Res. Soc. Proc. 63, Pittsburgh, PA, 1986).
12. Interatomic Forces in Relation to Defects and Disorder and Condensed Matter, edited by A. B. Lidiard, Phil. Magazine A **58** , No. 1 (1988).
13. Atomic Scale Calculations in Materials Science, edited by J. Tersoff, D. Vanderbilt and V. Vitek (Mater. Res. Soc. Proc., Vol. **141**, Pittsburgh, PA, 1989).
14. Atomistic Simulation of Materials: Beyond Pair Potentials, edited by V. Vitek and D. J. Srolovitz (Plenum Press, New York, 1989).
15. J. Th. M. DeHosson, in Interatomic Potentials and Lattice Defects, edited by J. K. Lee (The Metallurgical Society of AIME, Warrendale , PA, 1981), p.3.
16. R. Taylor, Physica B+C **131**, 103 (1985).
17. J. Hafner, From Hamiltonians to Phase Diagrams (Springer: Berlin, 1987).
18. M. S. Daw and M. I. Baskes, Phys.Rev.Lett. **50** 1285 (1983); Phys.Rev.B **29** 6443 (1984)
19. M. W. Finnis and J. E. Sinclair, Phil.Mag.A **50**, 45 (1984).
20. G. J. Ackland, G. Tichy, V. Vitek and M.W.Finnis, Phil.Mag.A, **56**, 735 (1987).
21. R. A. Johnson, Phys. Rev. B **37**, 3924 (1988).
22. A. E. Carlson, Solid Sate Physics, edited by H. Ehrenreich and D. Turnbull, Vol. **43**, p. 1 (1990).
23. J. A. Moriarty, Phys. Rev. B **38**, 3199 (1988); Phys. Rev. B, to be published (1990).
24. E. S. Machlin, in Theory of Alloy Phase Formation, edited by L. H. Bennett (The Metallurgical Society of AIME, Warrendale , PA, 1980), p. 127.
25. K. Maeda, V. Vitek and A. P. Sutton, Acta Metall. **30**, 2001 (1982).
26. V. Vitek and Y. Minonishi, Surf. Science **144**, 196 (1984).
27. G. J. Ackland and V. Vitek, Phys. Rev. B, May (1990).
28. G. J. Ackland, M. W. Finnis and V. Vitek, J.Phys.F **18**, L153, (1988).

29. G. J. Ackland and V. Vitek, in High-Temperature Ordered Intermetallic Alloys III, edited by C.T.Liu, A.I. Taub, N.S.Stoloff and C. C. Koch (Mater. Res. Soc. Proc., Vol. **133**, Pittsburgh, PA, 1986), p. 105.
30. V. Vitek, J. Phys. Appl. Paris, in press (1990).
31. S. M. Foiles, M. I. Baskes and M. S. Daw, Phys. Rev. B **33**, 7983 (1986).
32. R. Hultgren, R. L. Orr, P. D. Anderson and K. K. Kelley, Selected values of the Thermodynamic Properties of.Metals and Binary Alloys, (Wiley, New York, 1963).
33. M. J. Marcinkowski, N. Brown and R. M. Fisher, Acta Metall. **9**, 129 (1961).
34. S. M. L. Sastry and B. Ramaswami, Phil. Mag. **33**, 375 (1976).
35. R. Taylor, in Interatomic Potentials and Lattice Defects, edited by J. K. Lee (The Metallurgical Society of AIME, Warrendale , PA, 1981), p. 71.
36. J. Douin, P. Veyssiere and P. Beauchamp, Phil. Mag. A **55**, 565 (1987).
37. M. Yamaguchi, V. Paidar, V. Vitek and D. P. Pope, Phil. Mag. A **45**, 867 (1982).
38. M. Yamaguchi, D. P. Pope, V. Vitek and Y. Umakoshi. Phil. Mag. A **43**, 1265 (1981).
39. G. Tichy, V. Vitek and D. P. Pope, Phil. Mag. A **53**, 467 (1986).
40. D. P. Pope and S. S. Ezz, Int. Metals Rev. **29**, 136 (1984).
41. D. P. Pope and V. Vitek, in High-Temperature Ordered Intermetallic Alloys I, edited by C. C. Koch, C. T. Liu and N. S. Stoloff (Mater. Res. Soc. Proc., Vol. **39**, Pittsburgh, PA, 1985), p. 136.
42. V. Paidar, D. P. Pope and V. Vitek, Acta Metall. **32**, 435 (1984).
43. M. Yadogawa, D. M. Wee, Y. Oya and T. Suzuki, Scripta Metall. **14**, 849 (1980).
44. D. M. Wee, D.P.Pope and V.Vitek, Acta Metall. **32**, 829 (1984).
45. F. E. Heredia, G. Tichy, D. P. Pope and V. Vitek, Acta Metall. **37**, 2755 (1989).
46. G. Tichy, V. Vitek and D. P. Pope, Phil. Mag. A **53**, 485 (1986).
47. V. Vitek, Crystal Lattice Defects **5**, 1, (1976).
48. D. Farkas and E. J. Savino, Scripta Metall. **22**, 557 (1988).
49. M. H. Yoo, M. S. Daw and M. I. Baskes, in Atomistic Simulation of Materials: Beyond Pair Potentials, edited by V. Vitek and D. J. Srolovitz (Plenum Press, New York, 1989), p.401.
50. T. Takasugi , J. Phys. Paris **49**, C5-811 (1988).
51. C. T. Liu, in Interfacial Structure, Properties and Design, edited by M.H. Yoo, W.A.T. Clark and C.L. Briant (Mater. Res. Soc. Proc., Vol. **122**, Pittsburgh, PA, 1988), p. 139.
52. O. Izumi and T. Takasugi, J. Mater. Research **3**, 426 (1988).
53. C. L. Briant, J. Phys. France **49**, C5-3 (1988).
54. C. J. McMahon, Jr., in Grain Boundary Chemistry and Intergranular Fracture, edited by G. S. Was and S. M. Bruemmer, Mat. Sci. Forum **46**, 61 (1989).
55. J. J. Kruisman, V. Vitek and J. Th. M. DeHosson, Acta Metall. **36**, 2729 (1988).
56. S. P. Chen, D. J. Srolovitz and A. F. Voter, J. Mater. Res. **4**, 62 (1989).
57. V. Vitek, S. P. Chen, A. F. Voter, J. J. Kruisman and J. Th. M. DeHosson, in Grain Boundary Chemistry and Intergranular Fracture, edited by G. S. Was and S. M. Bruemmer, Mat. Sci. Forum **46**, 237 (1989).
58. E. M. Schulson, I. Baker and H. J. Frost, in High-Temperature Ordered Intermetallic Alloys II, edited by N. S. Stoloff, C. C. Koch, C. T. Liu and O. Izumi (Mater. Res. Soc. Proc. Vol. **81**, Pittsburgh, PA, 1987), p. 135.
59. A. H. King and M. H. Yoo, in High-Temperature Ordered Intermetallic Alloys II, edited by N.S. Stoloff, C.C. Koch, C.T. Liu and O. Izumi (Mater. Res. Soc. Proc. Vol. **81**, Pittsburgh, PA, 1987), p. 99.